Characterization of a Fresnel zone plate using higher-order diffraction

Akihisa Takeuchi,* Yoshio Suzuki and Hidekazu Takano

SPring-8, Mikazuki, Hyogo 679-5198, Japan.
E-mail: take@spring8.or.jp

The performance of a Fresnel zone plate has been tested by observing the focusing property of higher-order diffraction. The Fresnel zone plate was fabricated by the electron-beam lithography technique. The zone material was made from 1 μm-thick tantalum and the outermost zone width was 0.25 μm. The third-order focused spot size measured by the knife-edge scan method was 0.1 μm full width at half-maximum at an X-ray energy of 8 keV, which is exactly equal to one-third of the first-order focal spot size.

Keywords: Fresnel zone plates; higher-order diffraction; X-ray microbeams.

1. Introduction

Fresnel zone plates (FZPs) fabricated using lithography techniques are widely used for generating X-ray microbeams in the soft X-ray region. By using the high-precision electron lithography technique and a highly coherent X-ray beam from third-generation synchrotron radiation light sources, the best resolution achieved in the water-window region is better than 30 nm. On the contrary, FZPs in the hard X-ray region require a much thicker zone structure than that for the soft X-rays. Therefore, it is difficult to use a FZP dedicated to the soft X-ray region as it is. For example, the appropriate zone thickness for 10 keV X-rays is estimated to be about 2 μm even for high-density material (gold or tantalum). The accuracy of the electron-beam lithography technique is essentially the same as that for the fabrication process for soft X-ray zone plates. Therefore, when a zone plate of sufficient thickness can be fabricated, a high-resolution X-ray microbeam could be achieved even in the hard X-ray region.

Recently, zone plates designed for hard X-rays have been fabricated and applied to synchrotron radiation X-ray microbeams. Submicrometre beam sizes have been achieved (Yun *et al.*, 1999; Kagoshima *et al.*, 2000). At SPring-8, a FZP fabricated using the electron-beam lithography technique has been tested at undulator beamline 47XU. A focal spot size of 0.3 μm has been achieved by using a FZP with an outermost zone width of 0.25 μm (Suzuki *et al.*, 2001*a*). This spot size is almost equal to the diffraction-limited spot size for the first-order diffraction. The focal spot size obtained in the previous experiment is limited both by the diffraction and by the geometrical spot size due to the partially coherent illumination. Therefore, a finer focusing could be possible by utilizing higher-order diffraction at the expense of the diffraction efficiency, and the properties of higher-order diffraction could be a serious test of the accuracy of the zone structure. In this report, results of microbeam generation using third-order diffraction are described.

2. Experimental set-up

The FZP used in the experiment was fabricated using an electron-beam lithography technique at the NTT Advanced Technology (Ozawa *et al.*, 1997). The zone structure with an outermost zone width of 0.25 μm was made of 1 μm-thick tantalum. The diffraction limit for the first-order diffraction, defined as $1.22\,d_N$, was 0.3 μm. The diameter of the FZP was 100 μm, and the focal length for the first-order diffraction was 160 mm at an X-ray energy of 8 keV. A center beam stop (2.4 μm-thick gold) of diameter 50 μm was electroplated onto the FZP. Therefore, the diffraction limit for the spatial resolution determined by the width of the outermost zone and by the ratio of apodization (the radius of the center stop disc is half of the FZP radius) was 0.25 μm for the first-order focus (Born & Wolf, 1980). A schematic drawing of the FZP structure is shown in Fig. 1, and the specification parameters are listed in Table 1. The FZP was designed to have a zone ratio of 1:1. Therefore, the even-order diffraction was, in principle, the forbidden order.

Table 1
Specification of the Fresnel zone plate.

Diameter	100 μm
Designed focal length for first-order diffraction	160 mm at 8 keV
Outermost zone width (d_N)	0.25 μm
Diffraction limit (= $1.22\,d_N$)	0.3 μm for the first-order diffraction
Zone material	Ta, 1 μm-thick
Center stop	50 μm in diameter
Center-stop material	Au, 2.4 μm-thick
Supporting membrane	Si_3N_4, 2 μm-thick
Fabrication method	Electron-beam lithography at NTT-AT

The experiment was performed at beamline 47XU of SPring-8. A schematic diagram of the experimental set-up is shown in Fig. 2. A planar-type 139-pole undulator installed in the SPring-8 8 GeV electron storage ring was used as a light source. The magnetic period of the undulator was 32 mm, and the maximum K value of 2.3 was achieved by using in-vacuum permanent-magnet technology. The stored electron beam current was 100–80 mA during the experiment. The undulator radiation was monochromated at 8 keV by passing through a liquid-nitrogen-cooled Si 111 double-crystal monochromator. Both the first crystal and the second crystal of the monochromator were cooled by liquid nitrogen, and kept at the same temperature in order to achieve a fixed-exit-beam condition.

The monochromatic X-ray beam impinged on the FZP and was focused at the sample position. The distance between the light source and the experimental station was about 47 m. No optical elements except for the crystal monochromator were placed between the light source and the FZP. In the vertical direction, the microfocus beam was generated by producing a demagnified image of the light source. The vertical source size was very small because of the low coupling constant of the storage ring. The estimated source dimension in the vertical direction was about 20 μm full-width at half maximum (FWHM). However, the effective source size was broadened by vibration of the monochromator crystal. This vibration was estimated to be about 1 μrad. Therefore, the effective source size was considered to be about 100 μm in the vertical direction.

On the contrary, the horizontal source dimension (about 0.9 mm FWHM) was much larger than the vertical source size. Therefore, as

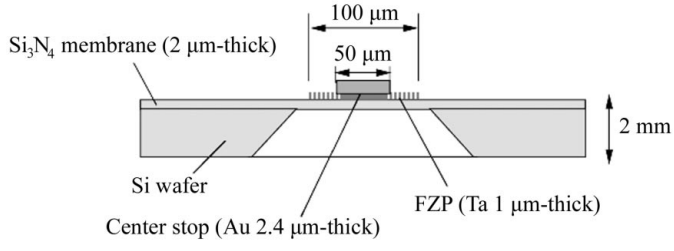

Figure 1
Schematic cross-sectional drawing of the FZP.

shown in Fig. 2, a vertical slit with an opening of 10 μm was placed between the monochromator and experimental station. The distance between the slit and the FZP was 9 m. The slit was used as a pseudo-point-like source in the horizontal direction, and a demagnified image of the slit was generated at the focal point. In this experiment, closer investigation has been carried out only on the horizontal focus because the effective source size in the vertical direction is not sufficiently small for generating the diffraction-limited focus in the present experimental condition.

In this optical system, the source location is not the same for the vertical and horizontal foci. Therefore, a kind of astigmatism exists in spite of the axial symmetry of the FZP. The focal length of the FZP for 8 keV X-rays was 160 mm for the first-order diffraction and $160/3 \simeq 53.3$ mm for the third-order diffraction. When the focal length of the optical element was 53.3 mm, the focal points were separated from each other by about 0.3 mm in the longitudinal direction. This separation of foci results in a spot size of 0.6 μm. However, this astigmatism is not a serious problem for the evaluation of optical elements. This is because the focusing property (resolution limit) is evaluated by measuring the line-spread function by means of a knife-edge scan. The focusing property in the horizontal and vertical directions can be tested separately using this configuration.

A pinhole (20 μm in diameter) made in a 0.2 mm-thick Ta plate was placed between the FZP and the focal point in order to select the third-order diffraction. The size of the order-selecting pinhole to discriminate the desired order of diffraction was determined by the focal length and the ratio of the center stop of the FZP.

As shown in Fig. 3(*a*), if a focal spot at a focal length f needs to be separated from the lower-order diffraction with a focal length f', the order-selecting pinhole has to be placed between the focal point at f and a point A. From a simple geometrical consideration, the diameter of the pinhole, d_0, must satisfy the following formula,

$$d_0 < d_1(f' - f)/(f - fd_1/d_2),$$

where d_1 and d_2 are the diameters of the center stop and the FZP, respectively. The above condition also determines the maximum working distance (pinhole-to-sample distance) for an appropriate pinhole size.

On the other hand, the diameter of the order-selecting pinhole also needs to satisfy the following formula in order to remove the higher-order diffraction, as shown in Fig. 3(*b*),

$$d_0 < d_1(f' - f)/f.$$

The condition $d_0 = d_1(f' - f)/f$ or $d_0 = 0$ is available when the pinhole is placed at the focal point. However, the pinhole usually needs to be placed at some distance from the focus. Therefore, the pinhole size optimized for the longest working distance (point B in Fig. 3*b*) is determined by following formula,

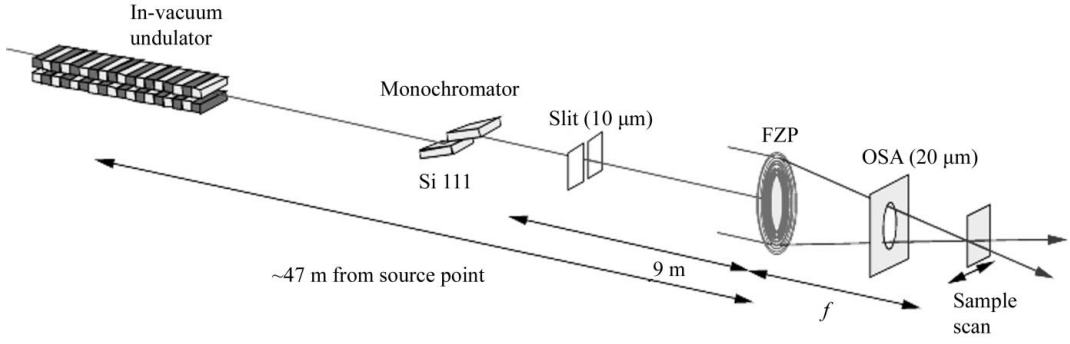

Figure 2
Schematic diagram of the experimental set-up. FZP: Fresnel zone plate; OSA: order-selecting aperture. $f \simeq 53.3$ mm at 8 keV for third-order diffraction. Effective source size: ~100 μm (vertical, 47 m from FZP), 10 μm slit (horizontal, 9 m from FZP). FZP material: Ta, 1μm-thick. Outermost zone width: 0.25 μm. Center stop: gold, 2.4 μm-thick, diameter 50 μm.

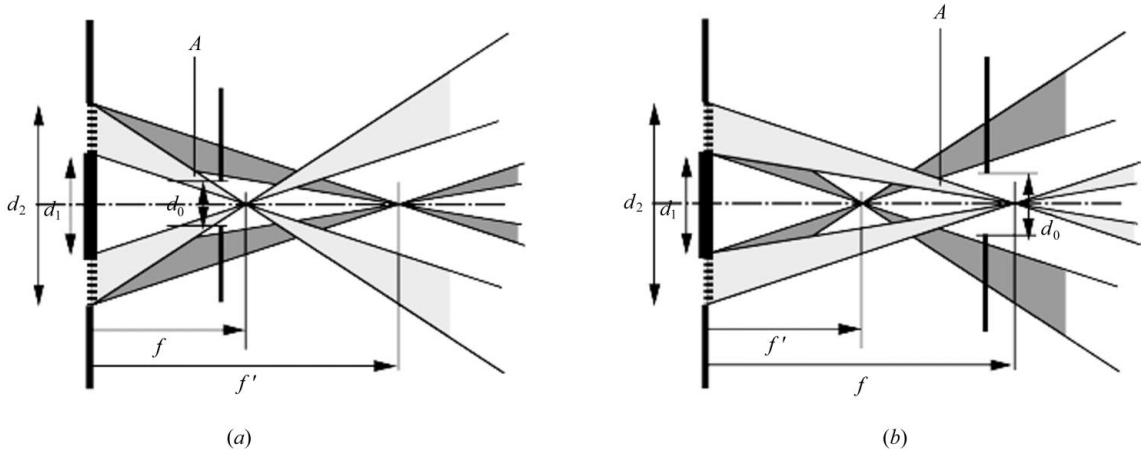

Figure 3
Geometrical configuration of the order-selecting aperture. (*a*) Removal of lower-order diffractions. (*b*) Removal of higher-order diffractions.

$$d_0 = d_1(f' - f)/(f' + fd_1/d_2).$$

In the present experiment, d_1 (diameter of the center beam stop) was 50 μm and d_2 (outermost diameter of the FZP) was 100 μm. The focal length for the first-order diffraction was 160 mm because an X-ray energy of 8 keV was used. In order to select only the third-order diffraction spot, the following conditions on the order-selecting aperture size must be satisfied:

$d_0 < 25$ μm, for removal of the first- and second-order diffraction beams;

$d_0 < 16.7$ μm, for removal of the fourth order;

$d_0 < 33.3$ μm, for removal of fifth and higher orders.

Therefore, the 20 μm-diameter pinhole used in the present experiment is not sufficient to remove the weak fourth-order diffraction which exists due to the imperfection of the ratio of even and odd zones.

It is also a problem that the thickness of the center beam stop (2.4 μm-thick gold adding to the 1 μm-thick tantalum) is not sufficient to stop the zeroth-order light. The transmittance of the center beam stop is 28% at 8 keV. Therefore the intensity of the transmitting beam (zeroth order) through the order-separating aperture of diameter 20 μm is about 1% of the incident radiation. The theoretical efficiency of the third-order diffraction is 2% for 1 μm-thick tantalum zone at 8 keV. Therefore the broad background due to the zeroth-order beam is not negligible when measuring the higher-order diffraction. These problems are, however, not so serious for the purpose of evaluating the focused beam profiles.

The diffraction-limited focused spot size for the third-order diffraction is one-third of that for the first-order diffraction. Therefore a focused spot size of 0.08 μm is expected if the illuminating beam is perfectly coherent. However, the focal spot size is also limited by the geometrical optics, *i.e.* a product of source size and magnification. The magnification (M) is defined by the equation $M = f/L$, where f is approximately equal to the focal length of the FZP ($\simeq$ 53.3 mm for the third-order focus) and L (9 m for the horizontal focus) is the distance between the source point and the FZP. The focal spot size determined by the geometrical optics is 0.06 μm in the horizontal direction for a focal length of 53.3 mm. This is smaller than the diffraction-limited resolution.

The focused beam profile was measured by the conventional knife-edge scan method. A mechanical translation stage driven by a stepping motor was used for the knife-edge scanning. Although the stage was a commercially available mechanical stage (Kohzu Seiki), an accuracy better than 10 nm was achieved by an open-loop-control system (Suzuki *et al.*, 2001*b*). A gold wire of diameter 50 μm was used as the 'knife edge'. The intensity of the monochromator output beam was monitored by an ionization chamber (air 1 atm), and the intensity of the focused X-ray beam was measured with another ionization chamber (air 1 atm). The line-spread function of the focused beam was derived from the numerical differential of the measured knife-edge scan profiles.

3. Results and discussion

The results of the focused beam profile measurement at an X-ray energy of 8 keV are shown in Fig. 4. As discussed in the above section, an intense and extremely broad background exists in the measured beam profile. The ratio of the focused beam intensity to the background tail is about 1:1 for the integral intensity, as is observed in the edge-scan profile. However, a sharp peak formed by the third-order diffraction beam appears in the differential profile of the edge scan. The FWHM of the focused beam peak is 0.1 μm. The spot size is almost equal to the diffraction-limited spot size. The large background in the raw edge-scan profile hardly affects the focused beam profile because the flux density of the background is much lower than that of the third-order focal spot. The broad tail is considered to be due to the zeroth-order beam passing through the center stop and to the weak fourth-order diffraction.

A theoretical beam profile calculated using the Kirchhoff formula for diffraction is shown in Fig. 5. The theoretical beam profile, taking the geometrical broadening of 0.06 μm into account, is also shown. As shown in the figure, the width of the main peak is not affected by the imperfection of the illuminating beam coherence when the geometrical spot size is smaller than the diffraction limit of the focus. As shown in Fig. 6, the measured beam profile shows good agreement with the calculated profile. The width of the measured focal spot is almost equal to that of the calculated beam spot. Assuming the random errors of the zone boundaries, the tolerance for the zone

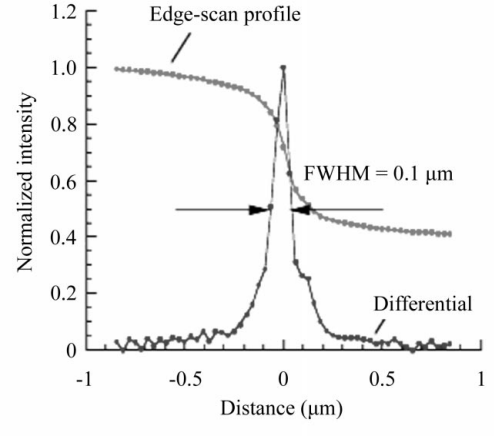

Figure 4
Focused beam profile for the third-order diffraction measured by knife-edge scan. The knife edge is scanned in 1/32 μm steps. Grey circles represent the raw data of the edge scan profile, and black circles represent the numerical differential of the edge-scan profile. The X-ray energy is 8 keV.

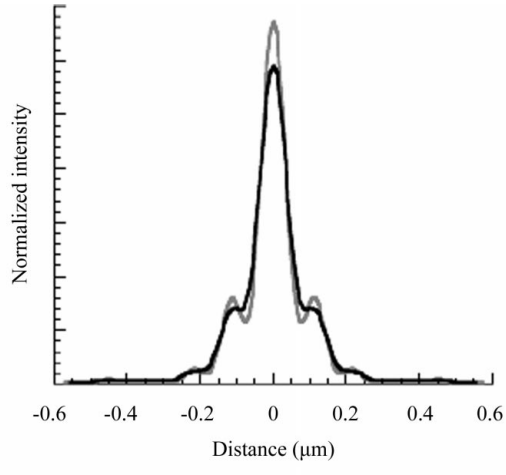

Figure 5
Theoretical line-spread function. Grey line: line-spread function for perfect coherent illumination. Black line: line-spread function for a geometrical spot size of 0.06 μm.

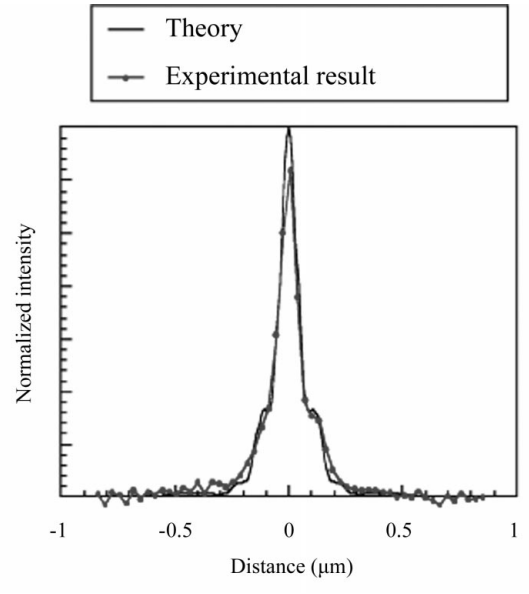

Figure 6
Comparison of the theoretical beam profile and the measured profile. The theoretical line-spread function includes a geometrical spot size of 0.06 μm. The weak background is subtracted from the experimental data, and the measured profile is normalized so that the integral of the beam profile is equal to that of the theoretical beam function.

boundary shifts for the diffraction-limited resolution is about 30% of the outermost zone width for the first-order focus and about 10% of the outermost zone width for the third-order focus (Simpson & Michette, 1983). Therefore, the experimental results suggest that the lateral structure of the FZP is fabricated within an accuracy of 25 nm.

References

Born, M. & Wolf, E. (1980). *Principles of Optics*, 6th ed., p. 416. New York: Pergamon.

Kagoshima, Y., Takai, K., Ibuki, T., Yokoyama, K., Takeda, S., Urakawa, M., Tsusaka Y. & Matsui, J. (2000). *X-ray Microscopy, Proceedings of the Sixth International Conference*, edited by W. Meyer-Ilse, T. Warwick & D. Attwood, pp. 668–671. New York: American Institute of Physics.

Ozawa, A., Tamamura, T., Ishii, T., Yoshihara, H. & Kagoshima, T. (1997). *Microelectron. Eng.* **35**, 525–529.

Shimpson, M. J. & Michette, A. G. (1983). *Opt. Acta*, **30** 1455–1462.

Suzuki, Y., Takeuchi, A., Takano, H., Ohigashi, T. & Takenaka, H. (2001*a*). *Jpn. J. Appl. Phys.* **40**, 1508–1510.

Suzuki, Y., Takeuchi, A., Takano, H., Ohigashi, T. & Takenaka, H. (2001*b*). *Proc. SPIE*, **4499**, 29–37.

Yun, W., Lai, B., Cai, Z., Maser, J., Legnini, D., Gluskin, E., Chen, Z., Krasnoperova, A. A., Vladimirsky, Y., Cerrina, F., Fabrizio, E. Di. & Gentili, M. (1999). *Rev. Sci. Instrum.* **70**, 2238–2241.

 Received 22 October 2001 • Accepted 12 March 2002